DOI: 10.1002/cssc.201100074

# Biomimetic Artificial Photosynthesis by Light-Harvesting Synthetic Wood

Minah Lee,[a] Jae Hong Kim,[a] Sang Hyun Lee,[b] Sahng Ha Lee,[a] and Chan Beum Park*[a]

In green plants, solar energy is collected by chlorophyll molecules and is passed on to photosynthetic reaction centers where it is used for oxygen evolution and carbon fixation.[1] During natural photosynthesis the energy, obtained from photons, of excited electrons generates a reducing power in the form of pyridine nucleotide cofactor, NAD(P)H, whose role as electron carrier is essential in reduction and oxidation reactions for photosynthetic cellular functions. The light-driven reduction of $CO_2$ to organic compounds occurs through the Calvin cycle, in which photochemically regenerated NAD(P)H is consumed by redox enzymes.[2] Inspired by natural photosynthesis, many efforts have been made towards the development of biomimetic artificial light-harvesting assemblies for making use of the practically unlimited supply of solar energy, and its conversion to chemical energy in different forms.[3–5] In particular, the light-induced cofactor recycling system has been regarded as a blueprint for biocatalytic reactions because $NAD(P)^+$/NAD(P)H-dependent redox reactions can be used to produce valuable fine chemicals.[6] Although redox enzymes are powerful biocatalysts for chemical synthesis, with high selectivity and catalytic efficiency under mild conditions, their applicability is limited by the high costs involved in supplying stoichiometric amounts of cofactor for industrial processes.[7–9] Several photochemical approaches, using "free" colloidal nanomaterials (e.g., p-doped $TiO_2$,[10] $W_2Fe_4Ta_2O_{17}$,[11] quantum dots[12]), have been reported for the visible-light-driven regeneration of NADH, but low efficiency and limited photostability due to reactive free radicals have hindered their practical application.[13]

Attempts to integrate photosynthetically active components within support materials, mimicking light-harvesting pigments embedded within thylakoid membranes of chloroplasts, have been reported.[14–17] The supporting matrix for encapsulation (or immobilization) of photosynthetic materials can assist in the organization of the guest materials and protect them by providing a stable microenvironment.[18] Furthermore, the approach allows easier handling of photoactive materials and facilitates recycling from the reaction mixture.[19] Herein, we provide the first report on light-harvesting synthetic wood (LSW) for biomimetic artificial photosynthesis. LSW can harness solar radiation for the regeneration of NAD(P)H, allowing the production of fine chemicals by NAD(P)H-dependant enzymes and mimicking the natural photosystem (Figure 1 A).

The porphyrins are a class of organic molecules that have a macrocyclic tetrapyrrole core that can be functionalized with different substituents. They exhibit remarkable photochemical, catalytic, electrochemical, and biochemical properties. The porphyrins include chlorophyll; the natural light-harvesting pigment (Figure 1 B).[20] In our LSW, porphyrins serve as light-harvesting pigments encapsulated within a porous lignocellulosic support. Encapsulation was achieved through simultaneous reactions: lignocellulose coagulation and porphyrin reprecipitation. The porous lignocellulosic support (SW) was a composite of three major structural components of plant cells: cellulose, hemicellulose, and lignin (Figure 1 C). In plant cells, crystalline cellulose microfibrils, which encapsulate cells in a mesh-like structure, are linked to hemicelluloses to provide strength as

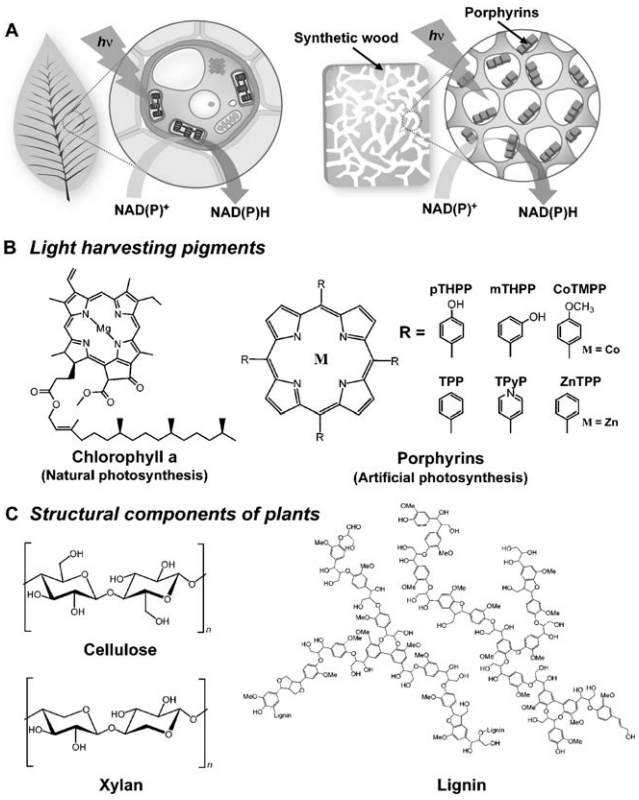


**Figure 1.** (A) Illustration of the light-harvesting system of green plants (left) and that of light-harvesting synthetic wood (LSW) (right). In both systems, light-driven cofactor regeneration takes place followed by NAD(P)H-dependant enzymatic reaction. (B) Molecular structures of light-harvesting pigment in plants (left) and LSW (right). (C) Molecular structures of structural components including cellulose, xylan, and lignin (tentative structure) common for plants and LSW.

[a] *M. Lee, J. H. Kim, S. H. Lee, Prof. C. B. Park*
*Department of Materials Science and Engineering*
*Korea Advanced Institute of Science and Technology*
*335 Science Road, Daejeon 305–701 (Korea)*
*Fax: (+82) 42-869-3310*
*E-mail: parkcb@kaist.ac.kr*

[b] *Prof. S. H. Lee*
*Department of Microbial Engineering*
*Konkuk University*
*Seoul, 143–701 (Korea)*

Supporting Information for this article is available on the WWW under http://dx.doi.org/10.1002/cssc.201100074.

  

well as extensibility, and lignin, a complex phenolic polymer, penetrates the voids, conferring mechanical strength to cell walls.[21] The all-wood composite is environmentally friendly and highly suitable for replacing nonrenewable, petroleum-based synthetic polymers. Furthermore, we found that the incorporation of lignin into SW is important for enhancing electron transfer in artificial photosynthesis.

The practical use of lignocellulosic materials has drawn much attention in response to growing environmental awareness, but their poor solubility in water has limited their application.[22] We used an ionic liquid to dissolve the unmodified lignocellulosic materials. Ionic liquids are chemically/thermally stable, nonflammable, and nonvolatile, so they have been considered as "green solvents."[23] The ionic liquid used in this study, 1-ethyl-3-methylimidazolium acetate ([$C_2$mim]OAc), in particular is known to have a low toxicity, low corrosiveness, and good biodegradability.[24] We obtained a SW gel film by removing [$C_2$mim]OAc from a preformed film of a viscous SW solution. As the film coagulated upon water treatment, [$C_2$mim]OAc was extracted from the film while the wood components barely dissolved in water, affording a translucent brown-colored gel (Figure 2A, inset). To characterize the inside structure of the SW film while minimizing collapse of the gel network, we removed water by freeze-drying. According to analysis by scanning electron microscopy (SEM) the SW has an interconnected macro- and mesoporous structure, which may lead to efficient mass transport during photosynthesis (Figure 2A). The pore-size distribution, obtained by Brunauer–Emmett–Teller (BET) analysis using $N_2$ adsorption, also indicated that the SW is mostly mesoporous, with a relatively broad pore-size distribution centered at ca. 20 nm (Figure 2B). The FTIR spectrum of the SW sample shows peaks typical for cellulose, xylan, and lignin (Figure 2C). The lignin peaks at 1513 $cm^{-1}$ and 1596 $cm^{-1}$ correspond to the aromatic skeletal vibration and the aromatic skeletal vibration breathing with C=O stretching, respectively.[25]

LSW capable of performing photosynthesis was prepared by encapsulating a hydrophobic porphyrin as photosensitizing pigment. We successfully incorporated water-insoluble porphyrins into SW by virtue of the strong solvating power of [$C_2$mim]OAc. Water was added to a porphyrin–SW solution, which was then casted as a film onto a glass plate to coagulate the lignocellulosic support. The hydrophobic porphyrins dissolved in [$C_2$mim]OAc were simultaneously entrapped in the SW gel through reprecipitation.

We tested six types of hydrophobic porphyrins, with different functionalities and metal centers (Figure 1B), for the visible-light-driven regeneration of NADH from $NAD^+$. Porphyrins with different substituents resulted in differential conversion yields (Figure 3A), and among the porphyrins, mTHPP showed the highest conversion yield of NADH; thus, mTHPP was chosen as a model porphyrin for further experiments. We did not observe leakage of the encapsulated mTHPP during immersion for more than 2 h in the reaction medium, according to changes in the absorbance spectra of the solution (Figure 3C, inset). This makes the LSW suitable for photoenzymatic reactions. We compared UV/vis absorption spectra of an mTHPP–SW solution and film to an SW solution and SW film (Figure 3C). The Soret band of the mTHPP–SW film was broader than that of mTHPP–SW solution. The $\lambda_{max}$ value (427 nm) of the Soret band of mTHPP–SW film was red-shifted by 5 nm compared to mTHPP–SW solution (422 nm) in [$C_2$mim]OAc. The small red-shift and broadening of the Soret band suggest changes in the molecular interactions of mTHPP entrapped in the film; a phenomenon commonly observed in spectroscopic studies on self-assembled monolayers[26–28] or supramolecular assemblies of porphyrins.[29] According to literature reports, the spectral change should be caused by the formation of J-aggregate-like, partially stacked structures that are adsorbed to the support by noncovalent interactions. Stacked face-to-face porphyrin aggregation (i.e., sandwich-type H-aggregates) is well-known to result in a spectral blue-shift relative to the mo-

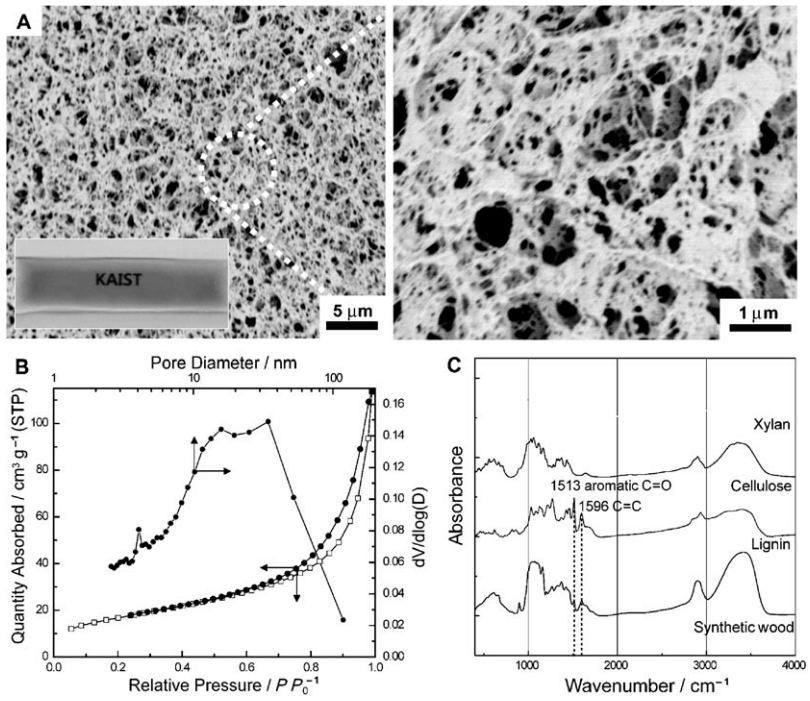


**Figure 2.** Characterization of the SW film. (A) SEM images of the SW film, showing its macro-/mesoporous structure. The inset is a photograph of the SW film, showing a translucent material (the sample has a brown color). (B) Nitrogen adsorption (open symbols) and desorption (filled symbols) isotherms, and Barrett–Joyner–Halenda (BJH) mesopore size distribution of SW (C) FTIR spectra of SW and its components (cellulose, xylan, and lignin).

  

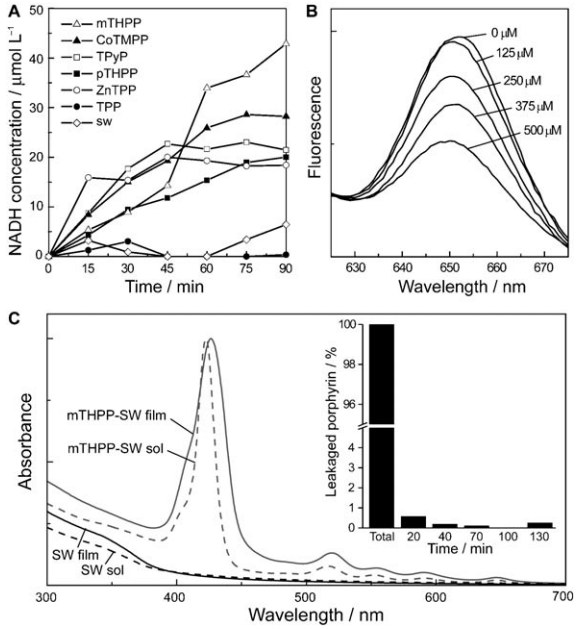


**Figure 3.** (A) NADH regeneration by water-insoluble porphyrins encapsulated in SW. mTHPP showed the highest NADH conversion yield. (B) Change in fluorescence of an mTHPP–SW film in the presence of **M** at various concentrations. (C) Absorption spectra collected from mTHPP–SW solution, mTHPP-SW film, SW solution, and SW film. The inset shows the amount of mTHPP leakaged from SW film over incubation time.

nomer excited-state level, whereas side-by-side porphyrin aggregation (i.e., J-aggregates) leads to a red-shift.[30] The relatively small red-shift of the Soret band compared to other porphyrin aggregates indicates moderate interaction among porphyrin molecules.[31,32]

For the visible-light driven NAD(P)H regeneration using mTHPP-SW, we used a rhodium-based organometallic compound, **M** ($[Cp^*Rh(bpy)H_2O]^{2+}$), as a hydride transfer mediator, instead of ferredoxin-$NADP^+$ reductase that works for NADPH photogeneration in natural photosynthesis. **M** is known to be capable of efficient regeneration of enzymatically active NADH as well as NADPH,[33–35] unlike ferredoxin-$NADP^+$ reductase which has specificity only for NADPH. For the SW–porphyrin hybrid material to facilitate artificial photosynthesis, the photoinduced electron-transfer reaction from porphyrin to **M** should occur efficiently, followed by a rapid reduction of NAD(P)H by **M**. To investigate the donor–acceptor relationship between mTHPP and **M**, we tracked changes in the fluorescence spectrum of mTHPP-SW film in the presence of **M**. As shown in Figure 3B, we observed a gradual decrease of the mTHPP fluorescence intensity with the increasing concentration of **M.** The emission quenching indicates that the presence of **M** inhibits the radiative decay of excited electrons in mTHPP, which should be due to the electron transfer from excited porphyrin to the electron acceptor **M**.[36,37] A detailed mechanism of NADH regeneration by **M** is shown in Figure S1 (Supporting Information).

To observe the effect of the SW composite on cofactor regeneration compared to pure cellulose, we tested the performance of porphyrins that demonstrated relatively high NADH regeneration efficiencies (TPyP, CoTMPP, and mTHPP, according to Figure 3A) in two different supports: SW film and cellulose film. As shown in Figure 4A, porphyrin–SW was much more efficient in NADH regeneration than porphyrin–cellulose. To investigate this difference, we measured photocurrents of mTHPP–SW film and mTHPP–cellulose film, each formed on ITO glass, in a 0.1 M phosphate buffer containing 15 w/v% triethanolamine (TEOA) over time intervals of 10 s by exposure to the light source. In response to the ON/OFF cycling of the light source, a stable, reproducible photocurrent was observed (Figure 4B). Furthermore, an increase in the net anodic photocurrent with an increase of positive bias to ITO electrode was observed (Figure 4C). These results indicate that the transfer of photoexcited electrons from mTHPP to the ITO electrode took place yielding the photocurrent generation, and the resulting oxidized mTHPP recaptured electrons from TEOA, an electron donor. From the photocurrent transients of the two films, we found that a higher photo-to-dark current ratio, as well as a faster response time, especially in the rise time, was achieved in the mTHPP–SW film. We attribute this result to improved charge transfer efficiency[38] by the introduction of lignin to the

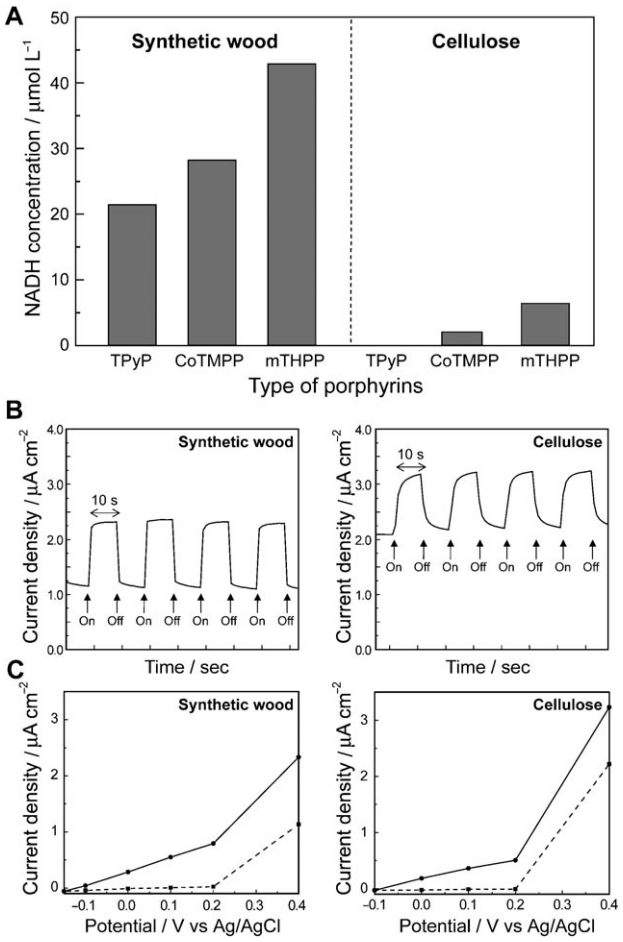


**Figure 4.** (A) Comparison between porphyrin–SW and porphyrin–cellulose films for photochemical NADH regeneration. (B, C) Photoelectrochemical properties of each film. The porphyrin–SW film shows enhanced performance in NADH conversion and photocurrent generation with a high photo-to-dark current ratio and a faster response time.

  

composite, which should be responsible for the enhanced NADH regeneration by the porphryin–SW film. Lignin contains free phenolic groups that enable the polymer to undergo oxidation–reduction reactions.[39] These phenolic groups in lignin can be oxidized into electroactive quinine functionalities, facilitating reversible proton-coupled two-electron redox cycling according to a recent report.[40] Furthermore, Barsberg et al. also suggested the existence of donor–acceptor interactions between the substructures in disordered lignin polymers.[41] Thus, similar to the protein environment of the natural photosynthetic reaction center in the thylakoid membrane containing electron donor and acceptor assemblies, such as plastoquinon and tyrosin residue involved in electron transfer,[42] the local environment of encapsulated porphyrin in LSW comprising lignin may energetically contribute to efficient charge transfer for biomimetic artificial photosynthesis.

As a mimic of the organic synthesis in the Calvin cycle by NAD(P)H-dependent redox enzymes, we combined a redox enzymatic reaction by L-glutamate dehydrogenase (GDH), a NADH-dependent oxidoreductase, with visible-light-driven cofactor regeneration facilitated by using LSW. An energy level diagram of our artificial photosynthesis system is illustrated in Figure 5A. The highest occupied molecular orbital (HOMO) ($E\sim-5.90$ eV) and lowest unoccupied molecular orbital (LUMO) ($E\sim-3.69$ eV) levels of mTHPP were estimated from cyclic voltammograms of mTHPP in DMSO (Figure S2). Visible-light-driven electron transfer reaction from the porphyrin to the electrochemical mediator (**M**) ($E\sim-3.96$ eV[43]) results in activation of **M**, which can transfer one hydride ion to NAD(P)$^+$ ($E\sim-4.2$ eV[7]) in one step (Figure S1). The electrochemical activation of the complex is achieved by two reduction steps followed by protonation.[44] Meanwhile, a sacrificial electron donor TEOA ($E\sim-5.37$ eV) reduces the oxidized porphyrin to avoid photodegradation of the dye. The regenerated cofactor NADH in an enzymatically active form is then consumed by GDH for the conversion of α-ketoglutarate to L-glutamate. It was observed that while the enzymatic synthesis of L-glutamate hardly occurred under dark stage, a gradual increase of conversion yield up to 18% was observed with the light on in 8 h (Figure 5B). The turnover frequency of mTHPP encapsulated in LSW was estimated to be ca. 1.25 $h^{-1}$, indicating a better efficiency than inorganic materials (e.g., p-doped $TiO_2$,[10] $W_2Fe_4Ta_2O_{17}$,[11] quantum dots[12]) reported for photochemical NADH regeneration. As expected, a control experiment with SW without encapsulating mTHPP did not show L-glutamatic synthesis (Figure S3). We found that the photoenzymatic conversion yield was affected by the composition of SW (Figure 5C). The conversion yield increased with increasing amounts of lignin, whereas hemicellulose did not show any notable effect on the synthetic reaction. This supports that lignin is involved in the electron transfer, improving the light-harvesting reaction. Taken together, our results show that SW can not only act as a supporting matrix for light-harvesting pigments, but can also enhance the photosynthetic reaction by the presence of lignin. LSW exhibited a high structural stability (Figure S4) and photostability (Figure S5), indicating that LSW is active for the overall photosynthetic reaction.

In summary, we demonstrated the development of an integrated artificial photosynthetic system by reassembling raw materials from plants as a support for the encapsulation of light-harvesting pigments. Similar to the natural light-harvesting by chloroplasts, water-insoluble porphyrins encapsulated in a lignocellulosic matrix enabled the utilization of light energy towards the photochemical regeneration of NADH cofactors and enzymatic chemical synthesis. The porous SW composite provides a microenvironment for porphyrin encapsulation and also allows an effective photosynthesis because of the inclusion of the redox-active lignin component. This work hints at a rational design of an artificial photosynthetic system by allowing the use of renewable natural biopolymers, facile fabrication under mild conditions, and an environmentally friendly process.

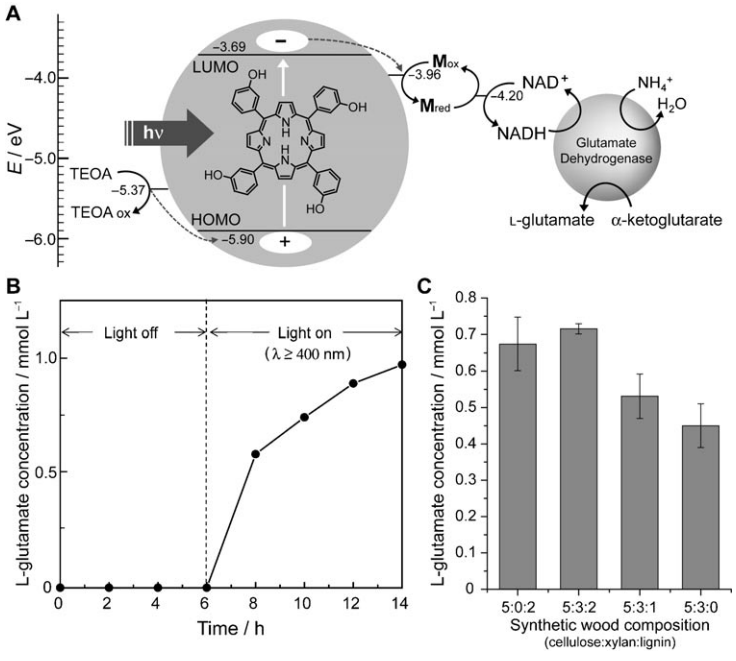


**Figure 5.** (A) Schematic energy-level diagram of the biomimetic artificial photosynthesis system. Under visible-light irradiation, photo-excited electrons of mTHPP encapsulated in LSW are transferred to **M**, generating reduction potentials for NAD(P)H regeneration. The dotted arrows refer to photo-induced electron transfer. (B) Time-profile of L-glutamate conversion yield under dark stage for 6 h, followed by a light stage for 8 h. (C) Effect of synthetic wood composition on L-glutamate conversion. The result shows a significant role of lignin in the photosynthesis of L-glutamate.

## Experimental Section

Materials: All chemicals, apart from porphyrins, were purchased from Sigma–Aldrich (St. Louis, MO, USA) and were used without further purification. Porphyrins including 5,10,15,20-tetrakis(4-hydroxyphenyl)-21H,23H-porphine (pTHPP), 5,10,15,20-tetrakis(3-hydroxyphenyl)-21H,23H-porphine (mTHPP), 5,10,15,20-tetrakis(4-methoxyphenyl)-21H,23H-porphine cobalt(II) (CoTMPP), 5,10,15,20-tetraphenyl-21H,23H-porphine (TPP), 5,10,15,20-tetra(4-pyridyl)-21H,23H-porphine (TPyP), and 5,10,15,20-tetraphenyl-21H,23H-porphine zinc (ZnTPP)

  

were obtained from Frontier Scientific (Logan, UT, USA). The organometallic rhodium complex **M**, pentamethylcyclopentadienyl-2,20-bipyridine-chloro-rhodium(III), was synthesized according the method by Kolle and Gratzel.[33–35]

Synthetic wood film formation: SW components including cellulose (2.5%, *w/w*), xylan (1.5%, *w/w*), and lignin (1%, *w/w*) were added to [$C_2$mim]OAc. The mixture was heated on a hot plate at 70 °C with vigorous magnetic stirring for more than 3 h to ensure the formation of a homogeneous solution. After complete dissolution, the resulting solution was spread on a glass plate and cast into a thin film with a thickness at 500 μm by a blade coating method. Deionized water was sprayed on the surface of the film to fix the shape. The sample was further immersed in water to precipitate a SW gel, followed by thorough washing for the complete removal of [$C_2$mim]OAc. For the synthesis of porphyrin-encapsulated SW films, or LSW, porphyrin solutions were prepared by dissolving porphyrins in [$C_2$mim]OAc at a concentration of 5 mg mL$^{-1}$ and mixed with the SW solution in the ratio of one to two. The resultant solution was stirred vigorously to ensure a homogenous distribution of porphyrin. Then, LSW films were formed using the solution according to the same method described above.

Characterization: The morphology of SW film was examined by using an S-4800 field-emission scanning electron microscope (SEM) (Hitachi High-technologies Co., Japan) at an acceleration voltage of 10 kV after Pt-coating by a SCD005 Pt-coater (Bal-Tec AG., Liechtenstein). Nitrogen adsorption-desorption isotherms were obtained by using a Surface Area and Porosity Analyzer ASAP2020 (Micromeritics, USA) at 77 K. Specific surface areas were calculated by using the BET equation in a relative pressure range between $P/P_0 = 0.05$–0.3. The pore-size distribution was estimated from the desorption branch of the isotherm by using the BJH method. FTIR spectra were obtained for the samples in KBr pellets by using a FT/IR-6100 (JASCO, Japan) at a resolution of 4 cm$^{-1}$ by taking 100 scans per spectrum. UV/vis absorption spectra of film or solution were measured by using a V-650 spectrophotometer (JASCO, Japan). Spectrofluorometric experiments were performed by using RF-5301PC (Shimadzu Co., Japan) with excitation wavelength of 430 nm.

Photochemical cofactor regeneration: The photochemical regeneration of NADH was conducted in a quartz reactor at room temperature under visible light. We used a 450 Watt Xe-lamp (Oriel Co.) equipped with a 400 nm cut-off filter as a light source. The reaction solution was composed of 1 mM $NAD^+$, 0.25 mM **M**, 15 w/v% TEOA in a 100 mM phosphate buffer (pH 7.4). LSW film prepared on a glass substrate was immersed in the reaction solution for NADH regeneration. The concentration of regenerated NADH was measured according to the increase in the absorbance of NADH at 340 nm by using BioSpec-mini spepctrophotometer (Shimadzu Co., Japan). Photocurrents were obtained by using a potentiostat/galvanostat (WonATech, Model: WMPG1000, Korea) with the predetermined applied potential (vs. Ag/AgCl) under the irradiation of a 450 Watt Xe-lamp equipped with the 400 nm cut-off filter. A 3-electrode system including mTHPP-SW or mTHPP-cellulose coated indium tin oxide (ITO) glass (working electrode), Ag/AgCl (reference electrode, 0.197 V versus normal hydrogen electrode), and a platinum wire (counter electrode) were connected to a multi-channel potentiostat/galvanostat. A phosphate buffer (100 mM, pH 7.4) with 15 w/v% TEOA was used as an electrolyte solution. Cyclic voltammograms of mTHPP was obtained with the same system except the working electrode, a glassy carbon disk (working diameter 2 mm), and the supporting electrolyte, a solution of 0.10 M TBAP in DMSO.

Enzymatic photosynthesis: The photosynthesis of L-glutamate was performed under visible light ($\lambda > 400$ nm) in an enzymatic reaction solution containing $NAD^+$ (0.2 mM), **M** (500 mM), α-ketoglutarate (5 mM), ammonium sulphate (100 mM), TEOA (15 w/v%), and L-glutamate dehydrogenase (40 unit) in a 100 mM phosphate buffer (pH 7.4). A constant flow of argon gas was supplied to the solution. For the quantitative analysis of L-glutamate, high-performance liquid chromatography (LC-20 A prominence, Shimadzu Co., Japan), using an Inertsil C18 column (ODS-3 V, length, 150 mm), was used. Samples were eluted by using phosphoric acid (0.05%) at the flow rate of 1.0 mL min$^{-1}$ and detected at 214 nm.

## Acknowledgements

*This study was supported by the National Research Foundation via National Research Laboratories (R0A-2008–000–20041–0), Converging Research Center (2009–0082276), and Engineering Research Center (2008–0062205) programs, Korea. This research was also partially supported by the EEWS initiative (KAIST).*

**Keywords:** biomimetic synthesis · hybrid materials · natural products · photosynthesis · porphyrins

[1] W. Kuhlbrandt, D. N. Wang, *Nature* **1991**, *350*, 130–134.
[2] J. M. Berg, J. L. Tymoczko, L. Stryer, *Biochemistry*, 6th ed. W. H. Freeman, New York, **2007**, pp. 541–551.
[3] T. Nakashima, N. Kimizuka, *Adv. Mater.* **2002**, *14*, 1113–1116.
[4] K. Sugiyasu, N. Fujita, S. Shinkai, *Angew. Chem.* **2004**, *116*, 1249–1253; *Angew. Chem. Int. Ed.* **2004**, *43*, 1229–1233.
[5] A. Ajayaghosh, V. K. Praveen, C. Vijayakumar, *Chem. Soc. Rev.* **2008**, *37*, 109–122.
[6] R. Wichmann, D. Vasic-Racki, *Adv. Biochem. Engin. Biotechnol.* **2005**, *92*, 225–260.
[7] H. K. Chenault, G. M. Whitesides, *Appl. Biochem. Biotechnol.* **1987**, *14*, 147–197.
[8] A. Schmid, J. S. Dordick, B. Hauer, A. Kiener, M. Wubbolts, B. Witholt, *Nature* **2001**, *409*, 258–268.
[9] H. Zhao, W. A. van der Donk, *Curr. Opin.Biotechnol.* **2003**, *14*, 583–589.
[10] Q. Shi, D. Yang, Z. Jiang, J. Li, *J. Mol. Catal. B: Enzym.* **2006**, *43*, 44–48.
[11] C. B. Park, S. H. Lee, E. Subramaniam, B. B. Kale, S. M. Lee, J. O. Baeg, *Chem. Commun.* **2008**, 5423–5425.
[12] D. H. Nam, S. H. Lee, C. B. Park, *Small* **2010**, *6*, 922–926.
[13] F. Hollmann, I. W. C. E. Arends, K. Buehler, *ChemCatChem* **2010**, *2*, 762–782.
[14] C.-J. Liu, S.-G. Li, W.-Q. Pang, C.-M. Che, *Chem. Commun.* **1997**, 65–66.
[15] B. T. Holland, C. Walkup, A. Stein, *J. Phys. Chem. B* **1998**, *102*, 4301–4309.
[16] T. Itoh, K. Yano, Y. Inada, Y. Fukushima, *J. Am. Chem. Soc.* **2002**, *124*, 13437–13441.
[17] K. Okeyoshi, R. Yoshida, *Adv. Funct. Mater.* **2010**, *20*, 708.
[18] J. C. Rooke, C. Meunier, A. Leonard, B.-L. Su, *Pure Appl. Chem.* **2008**, *80*, 2345–2376.
[19] S. L. Jain, J. K. Joseph, F. E. Kuhn, O. Reiser, *Adv. Synth. Catal.* **2009**, *351*, 230–234.
[20] X. Gong, T. Milic, C. Xu, J. D. Batteas, C. M. Drain, *J. Am. Chem. Soc.* **2002**, *124*, 14290–14291.
[21] T. T. Teeri, H. Brumer, G. Daniel, P. Gatenholm, *Trends Biotechnol.* **2007**, *25*, 299–306.
[22] A. Pinkert, K. N. Marsh, S. Pang, M. P. Staiger, *Chem. Rev.* **2009**, *109*, 6712–6728.
[23] T. Torimoto, T. Tsuda, K. Okazaki, S. Kuwabata, *Adv. Mater.* **2010**, *22*, 1196-.1221.
[24] N. Sun, M. Rahman, Y. Qin, M. L. Maxim, H. Rodrguez, R. D. Rogers, *Green Chem.* **2009**, *11*, 646–655.
[25] S. Kubo, J. F. Kadla, *Biomacromolecules* **2005**, *6*, 2815–2821.

  

[26] H. Imahori, H. Norieda, Y. Nishimura, I. Yamazaki, K. Higuchi, N. Kato, T. Motohiro, H. Yamada, K. Tamaki, M. Arimura, Y. Sakata, *J. Phys. Chem. B* **2000**, *104*, 1253 – 1260.
[27] Z. Zhang, T. Imae, *Nano Lett.* **2001**, *1*, 241 – 243.
[28] H. Yamada, H. Imahori, Y. Nishimura, I. Yamazaki, S. Fukuzumi, *Adv. Mater.* **2002**, *14*, 892 – 895.
[29] M. Ohtani, P. V. Kamat, S. Fukuzumi, *J. Mater. Chem.* **2010**, *20*, 582 – 587.
[30] R. F. Khairutdinov, N. Serpone, *J. Phys. Chem. B* **1999**, *103*, 761 – 769.
[31] S. Okada, H. Segawa, *J. Am. Chem. Soc.* **2003**, *125*, 2792 – 2796.
[32] X. Li, Z. Zheng, M. Han, Z. Chen, G. Zou, *J. Phys. Chem. B* **2007**, *111*, 4342 – 4348.
[33] E. Steckhan, S. Herrmann, R. Ruppert, E. Dietz, M. Frede, E. Spika, *Organometallics* **1991**, *10*, 1568 – 1577.
[34] H. C. Lo, C. Leiva, O. Buriez, J. B. Kerr, M. M. Olmstead, R. H. Fish, *Inorg. Chem.* **2001**, *40*, 6705 – 6716.
[35] F. Hollmann, B. Witholt, A. Schmid, *J. Mol. Catal. B: Enzym.* **2002**, *19–20*, 167 – 176.
[36] D. M. Guldi, G. M. A. Rahman, N. Jux, N. Tagmatarchis, M. Prato, *Angew. Chem.* **2004**, *116*, 5642 – 5646; *Angew. Chem. Int. Ed.* **2004**, *43*, 5526 – 5530.
[37] D. Baskaran, J. W. Mays, X. P. Zhang, M. S. Bratcher, *J. Am. Chem. Soc.* **2005**, *127*, 6916 – 6917.
[38] Y. Han, G. Wu, H. Li, M. Wang, H. Chen, *Nanotechnology* **2010**, *21*, 185708.
[39] E. Adler, *Wood Sci. Technol.* **1977**, *11*, 169 – 218.
[40] G. Milczarek, *Electroanalysis* **2007**, *19*, 1411 – 1414.
[41] S. Barsberg, T. Elder, C. Felby, *Chem. Mater.* **2003**, *15*, 649 – 655.
[42] K. N. Ferreira, T. M. Iverson, K. Maghlaoui, J. Barber, S. Iwata, *Science* **2004**, *303*, 1831 – 1838.
[43] F. Hollmann, A. Schmid, E. Steckhan, *Angew. Chem.* **2001**, *113*, 190 – 193; *Angew. Chem. Int. Ed.* **2001**, *40*, 169 – 171.
[44] F. Hildebrand, C. Kohlmann, A. Franz, S. Lutz, *Adv. Synth. Catal.* **2008**, *350*, 909 – 918.

Received: February 7, 2011
Published online on April 19, 2011

  